available at www.sciencedirect.com

ScienceDirect

journal homepage: www.elsevier.com/locate/compag

Sun, wind and water flow as energy supply for small stationary data acquisition platforms

Raul Morais[a,b,*], *Samuel G. Matos*[b], *Miguel A. Fernandes*[b], *António L.G. Valente*[a,b], *Salviano F.S.P. Soares*[a,b], *P.J.S.G. Ferreira*[c], *M.J.C.S. Reis*[a,b]

[a] *CITAB, Centre for the Research and Technology of Agro-Environment and Biological Sciences, Quinta de Prados, 5001-801 Vila Real, Portugal*

[b] *UTAD, Universidade de Trás-os-Montes e Alto Douro, Quinta de Prados, 5001-801 Vila Real, Portugal*

[c] *SPL, Signal Processing Laboratory, Dept. Electrónica, Telecomunicações e Informtica/IEETA, Universidade de Aveiro, 3810-193 Aveiro, Portugal*

ARTICLE INFO

Article history:
Received 3 April 2007
Received in revised form
3 February 2008
Accepted 19 April 2008

Keywords:
Energy harvesting
Power management
Energy sources
Acquisition station
Precision agriculture

ABSTRACT

The deployment of large mesh-type wireless networks is a challenge due to the multitude of arising issues. Perpetual operation of a network node is undoubtedly one of the major goals of any energy-aware protocol or power-efficient hardware platform. Energy harvesting has emerged as the natural way to keep small stationary hardware platforms running, even when operating continuously as network routing devices. This paper analyses solar radiation, wind and water flow as feasible energy sources that can be explored to meet the energy needs of a wireless sensor network router within the context of precision agriculture, and presents a multi-powered platform solution for wireless devices. Experimental results prove that our prototype, the MPWiNodeX, can manage simultaneously the three energy sources for charging a NiMH battery pack, resulting in an almost perpetual operation of the evaluated ZigBee network router. In addition to this, the energy scavenging techniques double up as sensors, yielding data on the amount of solar radiation, water flow and wind speed, a capability that avoids the use of specific sensors.

1. Introduction

The energy necessary for the deployment of stand-alone wireless sensor networks in large, open fields still dominates the overall system budget (Rabaey et al., 2000). The harvesting of energy from the surrounding space to power these systems is a solution being explored by several authors, including Wang et al. (2006); Thomas et al. (2006); Cantatore and Ouwerkerk (2006) and Priya et al. (2005). These works cover areas such as irrigation control systems, weather and environmental monitoring, greenhouse control, animal identification and health monitoring. But to effectively attain perpetual operation further enhancements in energy scavenging and more efficient power conditioning methods are required. In the case of precision agriculture (PA), massive amounts of data (Moreenthaler et al., 2003; Wang et al., 2006) are gathered to estimate, for instance, a growth profile, which suggests that sensors or even complete acquisition systems should be installed close to the plant itself. This implies dense ad-hoc networks of wireless devices, sufficiently flexible to support the disparate sources of data that can be extracted from the plant and its surrounding environment (Stafford, 2000). Besides, the wireless network

* *Corresponding author*. Tel.: +351 259 350 372; fax: +351 259 350 300.
E-mail addresses: rmorais@utad.pt (R. Morais), smatos@utad.pt (S.G. Matos), miguelseia@gmail.com (M.A. Fernandes), avalente@utad.pt (A.L.G. Valente), salblues@utad.pt (S.F.S.P. Soares), pjf@ieeta.pt (P.J.S.G. Ferreira), mcabral@utad.pt (M.J.C.S. Reis).
0168-1699/$ – see front matter © 2008 Elsevier B.V. All rights reserved.
doi:10.1016/j.compag.2008.04.005

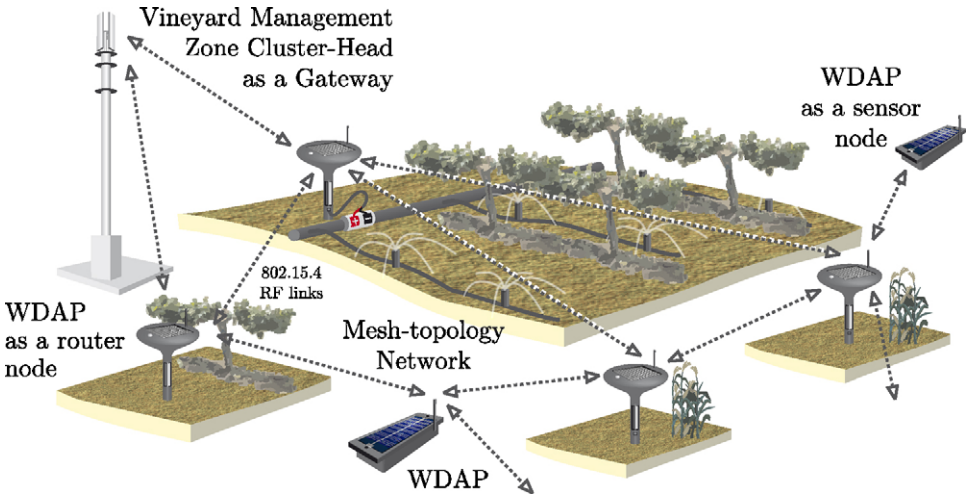

Fig. 1 – A perspective of our WDAP in a remote sensing application in a vineyard management zone. Each WDAP may operate as a router node in a ZigBee network to extend network coverage, acquiring and routing sensor data to a cluster-head as a sink node.

should be able to cover a large area, which means that each acquisition device should be capable of operating as a network router. Fig. 1 shows an illustration of our motivation scenario where a ZigBee network is deployed on a vineyard management zone to collect environmental data.

The harvested energy sources are usually ubiquitous in the nodes' surrounding space but random in nature (Paradiso and Starner, 2005; Hande et al., 2007), a characteristic that dictates the use of energy reservoirs, typically rechargeable batteries or, more recently, ultracapacitors (Park and Chou, 2006). In the case of wireless nodes operating as network routers the energy demands are considerable, and several sources of energy, possibly of different nature, may be required. This raises questions about the power density associated with such sources, how to harvest and manage them to achieve self-sustained, perpetual operation (Corke et al., 2007).

Design considerations regarding sensor networks, hardware design, network and medium access control protocols, battery management and harvesting techniques are discussed for instance in Raghunathan et al. (2005); Chou and Park (2005); Mainwaring et al. (2002) and Jiang et al. (2005). Dubois-Ferrière et al. (2006) describe TinyNode, a generic platform for wireless sensor network (WSN) applications, which operates with a small solar panel used to replenish two separate energy buffers (primary and secondary). Although not intended for perpetual operation, the authors present an interesting and useful comparison between supercapacitors and batteries for variable operation duty-cycle. They also present a comparison between current consumption of similar platforms, the Mica2, the Telos Sky, the EyesIFX and the TinyNode.

The solution to power indoor routers proposed by Hande et al. (2007) depends on a photonic energy harvesting device that consists of a set of solar cells connected in series-parallel to scavenge energy from 34 W fluorescent lights. However, the approach has drawbacks: on one hand, each router requires two nodes operating at 50% duty-cycle to minimise power consumption, a solution that duplicates the number of devices. On the other hand, it uses many solar cells that have to be located close to the lamps.

Chou and Park (2005) mention the need for multiple power sources, but they regard this power fragmentation problem as a consequence of the fact that such energy sources may not be available at all times. Park and Chou (2006) review the Helicomote, the Prometheus, the Everlast and the PUMA as energy harvesting systems and present the AmbiMax, an energy harvesting circuit that uses a solar panel and a wind generator to charge a supercapacitor-based energy storage system. In this case, the authors have focused their research in the harvesting efficiency rather than in controlling the charging process to avoid, for instance, the battery aging issue.

The goal of this paper is to demonstrate how to take advantage of the existence of multiple energy sources in agricultural and livestock environments (open-field crops, greenhouses, hydroponic and aquaculture systems, and stables) by harvesting energy from the sun, wind and moving water, as discussed in Section 2. The energy harvesters used in our experiments comprise a small solar-panel, a small hydro-generator placed in a nearby irrigation or hydroponic water pipe and a wind generator prototype that was designed to be part of the supporting structure of each acquisition platform. Section 3 describes the power-management behind a wireless data acquisition platform (WDAP) that uses the energy harvested from the three sources to simultaneously replenish a common 650 mAh NiMH battery pack, enabling almost perpetual operation of a network router with general-purpose data acquisition capabilities. Another feature of our approach, which complements the idea of harvesting from multiple sources, is to use the energy harvesting circuits as sensors of solar radiation and wind speed, which are relevant parameters in precision agriculture and other applications. This fusion or integration of the functions of generators and sensors makes conventional, separate sensors unnecessary. Regarding wireless network support, we have chosen (Morais et al., 2008) the ZigBee standard as a tool to create sensor an router nodes.

Section 4 describes our main experimental results: laboratory as well as outdoor experiments confirm the feasibility of self-sustained near-perpetual operation of our WDAP. For this purpose we have built two similar data acquisition systems, targeted for different applications, their main difference being the wireless support. Our results also show that the built-in sensors provide measures that are in good agreement with those of conventional, reference sensors. Our conclusions and final remarks are presented in Section 5, which closes the paper.

2. Harvesting energy from the environment

There is a variety of energy sources in the environment around a sensor network (Thomas et al., 2006; Paradiso and Starner, 2005) that are of potential interest for energy harvesting. They include photonic (includes solar energy as well as artificial lightning); vibrations (harvested using piezoelectric, electro-magnetic and capacitive converters); kinetic (available in moving water in rivers, pipes and wind flow); magnetic (magnetic fields surrounding AC power lines); pressure; and heat differentials (harvested using thermoelectric elements), where a comprehensive overview of these can be found in (Roundy et al., 2004). However, many of these sources may have to be neglected due to practical constraints or challenges raised by the low energy density, target power requirements and, in some cases, feasibility of the energy harvesting method.

Solar energy is the most efficient natural energy source available for sensor networks in outdoor applications (Thomas et al., 2006). An understanding of the relative importance and potential of solar and wind energy requires data on solar irradiation and wind velocity. The PVGIS (Photovoltaic Geographical Information System) on-line solar irradiation data utility, part of the SOLAREC action at the JRC Renewable Energies Unit of the European Commission (available at http://re.jrc.cec.eu.int/pvgis), collects such data. The results for a few locations in Europe are summarised in Table 1. It also includes wind data (the values for Vila Real were obtained by us, those for the other locations are available at http://www.windfinder.com).

The average horizontal irradiation for the city of Vila Real, northeast Portugal, is about 420.6 mWh/(cm^2 day). A network router device with a 40 mA continuous average current draw at 3.3 V would require an energy of about 3168 mWh/day, which can be harvested by a 10% efficient, 75.3 cm^2 solar panel. The active area of the solar panel has to increase to 215.1 cm^2 if we take the worst case value of 147.3 mWh/(cm^2 day) for the same location. If the solar panel inclination is optimal then the active area may be reduced to 130 cm^2.

Table 1 also shows the average wind speed and the probability that the wind velocity *exceeds* the Beaufort value 4, which corresponds to an average wind velocity of 5.5–7.9 m/s, or a median velocity of 6.7 m/s, over a 10-min interval (see also Fig. 2).

In the context of precision agriculture, and specially in hydroponic practices or close to irrigation systems, it makes sense to explore the kinetic energy from moving water. This can be harvested through a suitable hydro-generator and, as

Table 1 – Solar irradiation levels and wind statistics in different European locations

City	Optimal inclination angle (°)	Horizontal irradiation (mWh/(cm^2 day))			Irradiation at opt.incl. (Wh/(cm^2 day))			Average wind speed[a] (m/s)	Wind probability ≥ 4 Beaufort[b] (%)
		Min	Max	Average	Min	Max	Average		
Wageningen, Netherlands	36	45.5	479.9	265.5	73.8	476.6	302.0	5.7	48
London, UK	36	52.3	484.3	269.8	89.5	482.6	309.9	5.1	42
Paris, France	35	66.3	554.9	305.3	104.0	546.7	347.2	4.6	32
Vila Real, Portugal	34	147.3	680.6	420.6	243.9	656.7	482.9	5.5	> 35
Madrid, Spain	34	161.9	733.5	449.7	269.2	694.1	515.0	3.0	15
Lisbon, Portugal	33	190.0	704.1	447.5	315.2	663.5	509.7	4.6	34
Almeria, Spain	33	218.4	696.3	461.5	364.2	642.2	523.9	4.6	33

[a] Average wind speed, per year.
[b] The Beaufort scale refers to a subjective scale based on the impact of wind force on the environment. In this case, the value greater than 4 indicates the probability of the wind achieving a speed greater than 5.5 m/s.

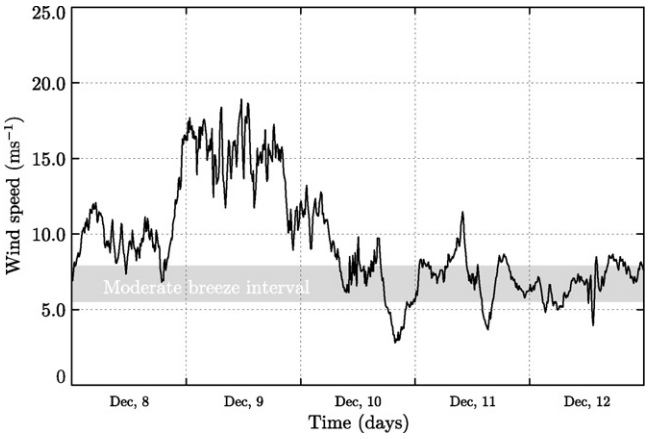

Fig. 2 – Results from wind measurements (2 m above ground) for a 5-day period. The wind speed was above 5 m/s for more than 90% of the period, a value that justifies kinetic energy harvesting by a small wind turbine.

we will see, it may considerably supplement the WDAP energy reservoir.

Our multi-source energy supply harvesting strategy, including the appropriate enclosure box, is illustrated in Fig. 3. The WDAP is used in a vineyard management zone to collect data from soil moisture, soil temperature, air temperature, relative humidity and solar radiation as a part of an on-going project. The energy is in this case supplied by sun, wind and moving water. In the latter case, the energy is harvested by a hydrogenerator located in a nearby irrigation pipe.

2.1. *Solar-energy harvesting*

Solar-energy harvesting is based on the well-known principle of photo-voltaic conversion, and provides the highest power density (15 $mWcm^{-2}$on a bright sunny day), making it the best-suited choice to power wireless acquisition systems in outdoor applications. Since the power output of small solar panels is limited, two main design principles for the solar-harvesting modules are considered. First, the system should extract the maximum power at each time instant and, second, the efficiency of the power management sub-systems should be maximised. In practice, strict adherence to these principles is difficult, and trade-offs have to be considered, due to the interaction of factors such as the characteristics of the solar cells and their active area, power conditioning features, application requirements of the wireless system and, the chemistry and capacity of the batteries used to store the harvested energy. But to maximise solar to electrical energy conversion efficiency the power conditioning subsystem should operate at the solar panels' maximum power point (MPP), the point in the *V–I* characteristic that corresponds to the maximum power transfer.

Our prototype, the MPWiNodeX platform, uses a commercial solar panel (MSX-005 from Solarex, USA) chosen because of its small size, availability and low cost. This 8-cell solar-panel has an active area of 57.0 mm × 95.8 mm (54.6 cm^2), a rated V_{oc} of 4.6 V and I_{sc} of 160 mA. The MPP occurs at a voltage of approximately 3.1 V, which means that the power conditioning circuit should ensure operation at (or near) this point.

Regarding the harvesting circuit, one approach is to clamp the output terminals of the solar panel to a rechargeable battery (Raghunathan et al., 2006). This forces the solar panel to operate at a point on its *V–I* curve determined by the battery's terminal voltage. This has the advantage of minimising the energy losses in the transfer mechanism, but depends on a careful choice of battery and solar panel in order to ensure that the operating point of the system remains close to the MPP. In the cited example, two NiMH batteries are charged, via a blocking diode, by a solar panel with

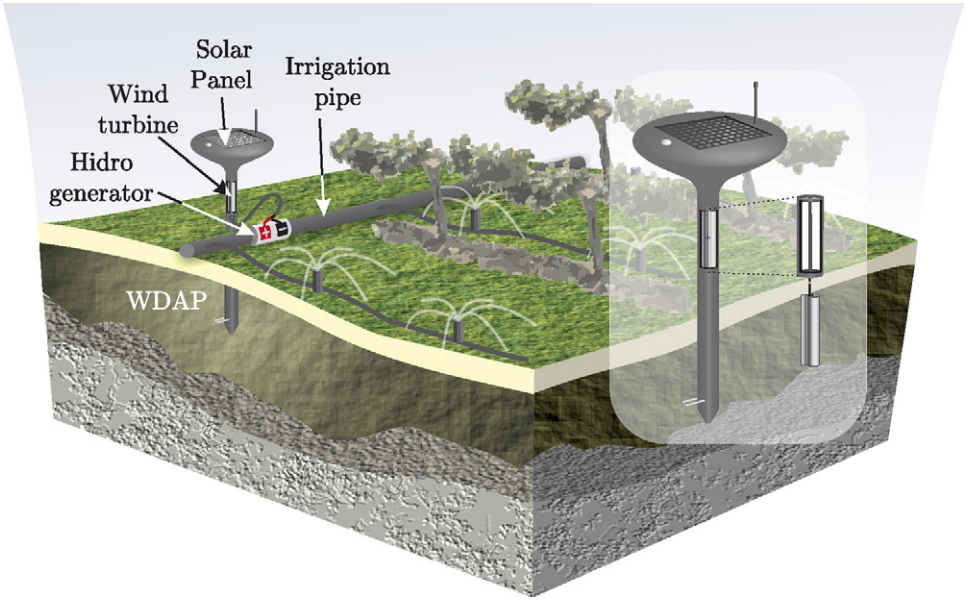

Fig. 3 – The concept of a multi-energy source applied to a self-standing WDAP. Energy is harvested by an embedded solar panel, a vertical axis wind turbine integrated in the supporting structure and a hydrogenerator installed in irrigation pipes.

a MPP occurring at 3.0 V. Battery voltage varies between 2.2 and 2.8 V, and due to the voltage drop in the blocking diode, the voltage across the solar panel remains close to optimal. It only harvests energy when the solar panel output voltage is 0.7 V higher then that of the battery which means that a significant amount of energy cannot be harvested. Moreover, there is no tracking of the MPP, which is essential to achieve high harvesting efficiency (Park and Chou, 2006). Also, the energy flow is unmanageable, resulting in uncontrolled daily recharge cycles and placing a significant stress on the battery.

Our solution represents an integrated approach to the management and conditioning of the solar-panel, wind generator and hydrogenerator blocks (described in the following two sections). It includes a smart-battery charge control that balances battery lifetime and energy harvesting efficiency, as described in detail in Section 3.1.

2.2. *Wind flow kinetic energy harvesting*

Wind flow kinetic energy can be harvested by a wind turbine which extracts energy from moving air by slowing it down and using the obtained energy to drive a generator. The power P_w associated with a quantity of air of mass m, flowing at speed v in the x direction, is the time derivative of the kinetic energy:

$$P_w = \frac{1}{2}\rho A \frac{dx}{dt} v^2 = \frac{1}{2}\rho A v^3, \quad (1)$$

where ρ is the air density in $kg\,m^{-3}$, A is the cross-sectional area in m^2 and v is the upstream or undisturbed wind speed in m/s. An ideal turbine can extract a fraction of the power in (1) given by the Betz coefficient 16/27 or 59.26% (Betz, 1926). The power extracted by a practical turbine is

$$P_m = C_p \tfrac{1}{2}\rho A v^3 = C_p P_w. \quad (2)$$

where C_p is the performance coefficient of the turbine. Assuming that the turbine is coupled to a transmission with efficiency η_m which drives a generator of efficiency η_g, the electrical power P_e available can be written as

$$P_e = C_p \eta_m \eta_g P_w = C_p \eta_m \eta_g \tfrac{1}{2}\rho A v^3. \quad (3)$$

Wind turbines can be classified into two general types based on the axis of rotation. Horizontal axis wind turbines (HAWT) have the rotor shaft parallel to ground and must be pointed into the direction of wind flow by some means. They are usually used for large-scale windmills for electrical energy production. Vertical axis wind turbines (VAWT) have a vertically rotating main rotor shaft. Although less efficient, VAWTs offer some important advantages in small-scale wind generator design, the Darrieus and Savonious designs being the most common. They are omni-directional, simpler, can be fixed in both ends and can respond quicker to changes in wind direction and velocity. The Darrieus type is based on lift forces which cause the rotor to move faster than the wind. They are efficient but usually not self-starting. The Savonious type is less efficient because they are drag-type devices (S-shaped cross section) but they are self-starting and virtually maintenance-free.

Fig. 4 – Small vertical axis wind turbines prototypes.

To design the wind generator suited for our application it is necessary to bear in mind a number of practical and functional issues. Firstly, the energy harvested from the wind is intended to supplement the energy available for battery charging. Secondly, the wind generator should double up as a sensor, and be capable of supplying data on wind speed. Finally, the wind generator should be part of the structure of the acquisition station and especially of the rod which stands vertically on the ground (right side of Fig. 3). This means that the turbine swept area, namely its diameter, should be minimised. To fulfil these requirements, a Savonious design was chosen, despite its inherent low efficiency. The power extraction coefficient could be increased by adding a convergent nozzle to increase the rotor speed (Shikha et al., 2003). However, this requires wind coming from a fixed direction, which is not the case in our application target. A free moving vane would force the convergent nozzle into the direction of the wind, and could be used to obtain information about wind direction. The efficiency can be improved in a more simpler way by adopting a multi-blade rotor design.

Fig. 4 illustrates the two VAWT that were constructed to evaluate the wind energy harvesting techniques. The right one is based on a six-blade Savonious design with 60 mm diameter and 200 mm height (0.012 m^2 swept area), while the left one is based on three-stage based design as proposed by Hayashi et al. (2005). Assuming air standard conditions(pressure of 101.3 kPa and temperature of 273 K) and a power coefficient C_p of 0.1, these turbines should extract a mechanical power of 97 mW at a wind speed of 5 m/s.

Fig. 5 – Photograph of the commercial hydrogenerator installed in a irrigation pipe.

2.3. *Water-flow kinetic energy harvesting*

The energy of moving liquids in pipes, such as water or liquid nutrients, can be harvested with a small-size hydrogenerator. To our best knowledge, this approach has not been explored to supply energy to small electronic devices in precision agriculture. We regard the pipes of irrigation control systems as power outlets within the crops. This idea may be even more relevant in aquaculture or hydroponics practices, where water is always recirculating in pipes. This suggests the possibility of supplying power to a sensor network based on the energy harvested from these pipes.

To explore and validate this concept, a commercial hydrogenerator was used as a energy harvester for our WDAP. This device, illustrated in Fig. 5, was developed and patented by Vulcano to replace batteries in smart gas-based water heating appliances for residential applications. With a principle of operation similar to large hydroelectric generation systems, a small quantity of water, derived from the main duct, is used to spin a turbine coupled to a DC generator. Fig. 6 shows the results of our experiments, conducted with the hydrogenerator for different values of inlet water flow. As can be seen, the hydrogenerator output voltage is almost constant and independent of the water flow value. Due to this characteristic, the water volume cannot be accurately measured, but its logical state can (flowing/not flowing, useful for detecting liquid movements).

3. System architecture

To evaluate the energy harvesting techniques as well as the data correlation between reference sensors and data gathered from the energy harvesters, two different WDAP were designed, differing mainly in wireless support. The first and simplest prototype, the MPWiNodeS variant, uses a low-cost 8-bit RISC μ-controller (PIC18LF2620 from Microchip, AZ, USA) and a low-power RF transceiver (RC1280 from Radiocrafts, Norway). This device is currently being used as a development platform for the inclusion of the IEEE 1451 standard for sensor/network interoperability (Wei et al., 2005; Sweetser et al., 2006), with the objective of defining the energy harvesters transducer electronic data sheet (TEDS). The second prototype, the MPWiNodeZ, uses a wireless μ-controller (JN5139 from Jennic, UK) with a ZigBee-compliant stack, and provides the necessary standardised software tools to rapidly deploy sensor and router nodes in the field. These devices follow the block diagram depicted in Fig. 7. A detailed explanation of the diagram is given in the following subsections.

3.1. *Power management*

The power conditioning subsystem (Fig. 8) is responsible for charging the NiMH battery pack with energy harvested from the three considered energy sources. Each source has its own conditioning block, based on a highly efficient boost converter with 3.3/5.0 V output voltage, pin selectable. This converter allows a wide range of input voltages below the battery nominal output, which enables harvesting from low-voltage sources. The shutdown pin is used to implement a pulse charging mechanism, which simultaneously performs MPP tracking to enhance harvesting efficiency. This signal is generated by a comparator with hysteresis powered by the

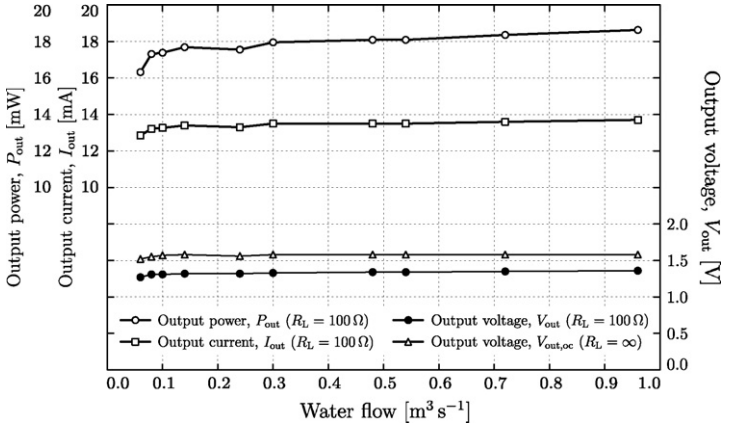

Fig. 6 – Output voltage and current of the hydrogenerator during an evaluation performed for several values of water flow. The electrical load was in this case a 100 Ω resistor. As expected, the output power is almost independent of the main duct water flow.

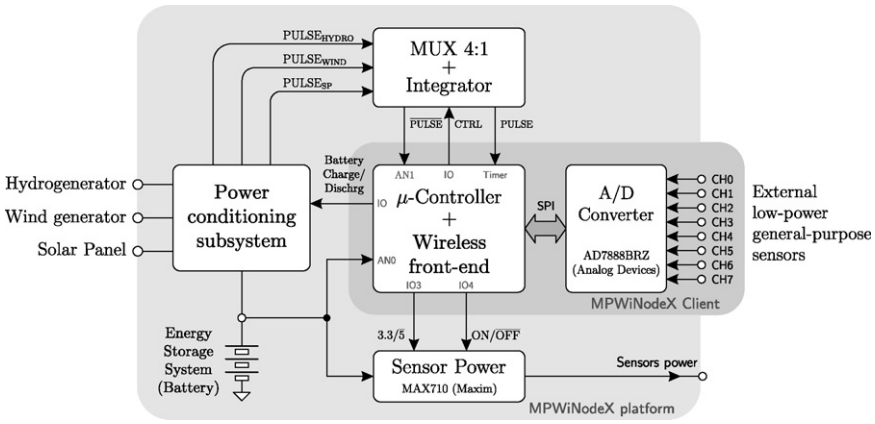

Fig. 7 – Block diagram of the WDAP and power management platform.

battery due to its ultra-low quiescent current. When the voltage at the charge reservoir capacitor (see Fig. 8) rises above a particular value, the comparator turns the boost converter on, transferring the charge stored at that capacitor to the battery, causing the input voltage to drop. Dropping below the lower-trip point of the comparator will result in the turn-off of the converter. This pulsed operation results in a more efficient charging method (Zhang et al., 2004), where the density of the generated shutdown pulses is related with the capability of the energy source to replenish the input charge reservoir. This relation is, in this work, explored to provide a coarse estimation of the magnitude of the parameter that supplies the energy to the system. To this effect, a second comparator with open drain output is used to generate similar yet independent pulses.

The other feature is the output voltage selection pin, used to select the 3.3 or 5.0 V predefined value, which are, in this case, below and above the operating limits of a 3-cell NiMH battery. This is used to define the start and stop conditions, battery charging and floating, respectively.

The systems' power supply is derived from a wide input range DC–DC converter (MAX710 from Maxim, USA). Among other features, it has a low-battery indicator (LBI signal in Fig. 8) that is used to signal the μ-controller when the battery voltage falls below a predefined value, suitable for predicting the power-off. The μ-controller is responsible for sampling the battery voltage value and to control the operation of the conditioning subsystem. When the battery achieves a pre-programmed value, which could be the battery fully charged (BFC) voltage value, a normally closed power switch is used to break the charging path. This switch may also be used for discharging completely the battery as a way to minimise the aging issue by periodically promoting, if necessary, a full discharge/charge cycle.

3.1.1. *Solar-panel power-conditioning block*

When conditioning solar energy, the boost converter described above is a more suited choice since it enables harvesting even in that cases that the solar panel output voltage is lower than the in-charging battery voltage level. As the internal resistance of the photovoltaic cells depends on the light levels, which causes a loss of efficiency when connecting it to the boost converters' inductor, the input charge reservoir capacitor introduces two important improvements. By monitoring the voltage on this capacitor, the comparator turns on the boost converter when the solar panel voltage output is at its MPP. The comparator will turn-off the converter without allowing the converter's input voltage to drop below its operating voltage limit. The turn-off condition will remain until the solar panel output voltage rises again to the optimum voltage. The input capacitor also provides a low-impedance path for the inductor current, which allows the efficient bang-bang control of charge transfer (Maxim, 2000). Fig. 9 illustrates the principle of operation of this bang-bang control, where it

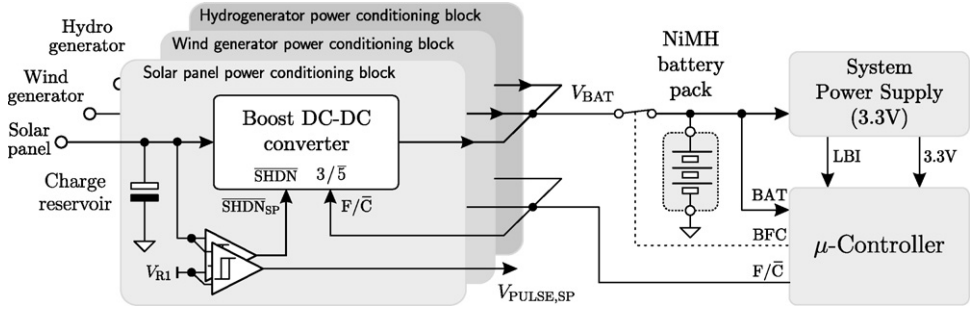

Fig. 8 – Functional diagram of the power-conditioning subsystem where each conditioning block contributes to the battery charging. The output signal from each block ($V_{PULSE,i}$) is available to give a coarse estimation of the parameter that supplies energy.

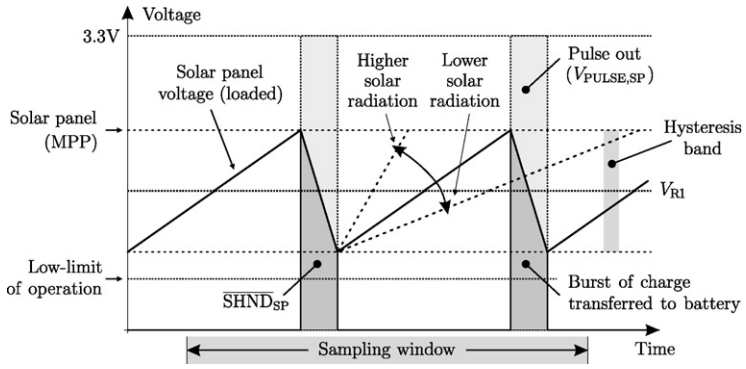

Fig. 9 – Charge transfer mechanism between the solar panel (operating at its MPP) and the battery, which yields data on amount of the energy source.

is also shown how the density of the charge transfer burst pulses are correlated with the received solar radiation intensity. It can be followed that the pulse density ($V_{PULSE,SP}$ in Fig. 9) increases as the solar irradiance rises, which we regard as a solar radiation sensor output.

3.1.2. *Wind generator and hydrogenerator power-conditioning blocks*

The wind generator is based on a four permanent magnet generator, which creates an alternating sinusoidal voltage with an amplitude and frequency proportional to the extracted wind mechanical power. Depending on the possible electrical connections that we can make with four windings, a rectifier is used before connecting this voltage source to the input of the power-conditioning block. A two-diode full-wave rectifier topology provides the higher electrical power extraction but causes more electromagnetic breaking, because current flows during the entire period. This leads to an equivalent higher starting torque when the DC value reaches the equivalent MPP. In other words, when the DC output from the generator reaches the ON switching condition of the boost converter, a higher current flows in all windings which causes breaking. To reduce this starting torque (enabling operation at lower speeds with the penalty of a lower efficiency) we have followed the half-wave rectifier approach to allow harvesting energy from low-speed winds. However, a power routing scheme can be implemented to switch from the half-wave to the full-wave rectifier mode whenever the wind speed is above a determined value.

Power conditioning of these two generators is accomplished by the same principle of operation of the solar-panel power-conditioning block. The differences are the values (resistors in this case) that define the MPP for each energy harvester. The wind generator and hydrogenerator high

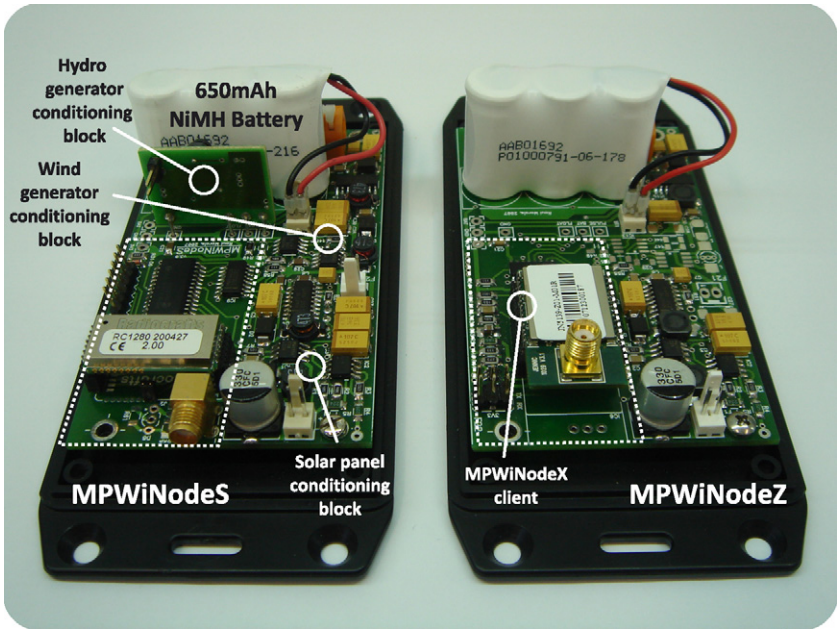

Fig. 10 – Photograph of the two developed WDAP as MPWiNodeX power-management platform clients. Inside the dashed rectangle is the core μ-controller (PIC18LF2680 at left for the S-variant and JN5139 for the Z-variant).

trip-values were set to approximately 2.0 and 1.6 V, respectively.

3.1.3. *Battery charge control*

The battery charging start and stop conditions are asserted by the μ-controller by means of the selection pin ($3/\bar{5}$) of each boost converter (see Fig. 8). To this effect, the battery voltage is sampled periodically to monitor when it becomes fully charged. When it happens, the μ-controller sets the $3/\bar{5}$ line which causes the boost converter to be turned off because the output voltage is greater than the selected predefined output voltage. If the battery is actually discharging, and its voltage drops below some predefined value, the μ-controller may clear the $3/\bar{5}$ pin, which starts, or resumes, a charging cycle.

At first sight, the selection of the switching points is straightforward. The voltage across a 3-cell NiMH battery should not exceed 3× 1.45 V = 4.35 V, where 1.45 V corresponds to a fully charged NiMH cell. To minimise battery aging, the discharge cycle should last until the voltage falls down to 3× 0.9 V = 2.7 V, where 0.9 V is the voltage across a completely discharged cell (Ying et al., 2006; Fetcenko et al., 2007). To avoid a fully discharged cell, even knowing that a residual energy may exist, we decided to limit the lower bound to a 3 V value.

Due to power fragmentation it becomes necessary to balance battery lifetime and energy harvesting efficiency. To better understand the need for the trade-off, consider that the battery is discharging, and that its voltage is, for instance, 3.7 V; assume now that, at this stage, an external unpredictable energy source becomes available. Should this fact be ignored and the battery be allowed to continue discharging until its voltage reaches 3.3 V? Or should the battery be recharged while the unpredictable energy source is present? It is clear that the strict maximisation of the battery lifetime implies the sub-optimal use of the harvested energy, and increases the probability of running out of power. On the other hand, any attempt to use as much harvested energy as possible might severely limit the duration of the batteries as a result of uncontrolled charging cycles. To overcome this issue, a software-based solution has been implemented. With access to the actual battery voltage value, a software procedure sets the trip voltage values so that complete discharge cycles can be periodically performed, thus yielding a

Fig. 11 – Experimental evaluation of the WDAP in a vineyard management zone. In this setup, the energy was supplied by the sun, wind and sporadically by irrigation water.

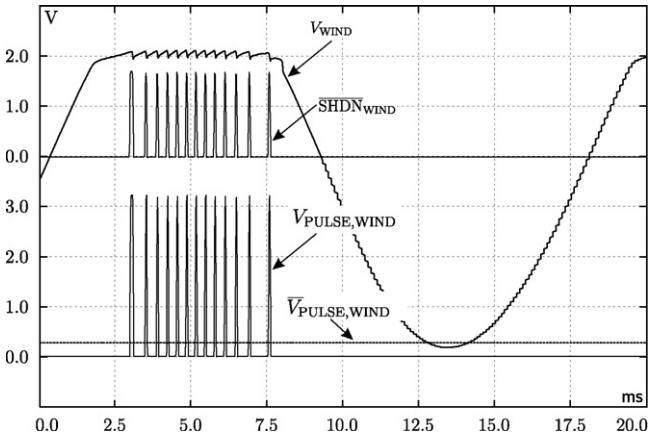

Fig. 12 – Wind generator power conditioning waveforms. The conditioning block maintains the wind generator working at its MPP ($V_{WIND} \approx 2$ V) resulting the $V_{PULSE,WIND}$ that is averaged to give a coarse estimation of wind speed.

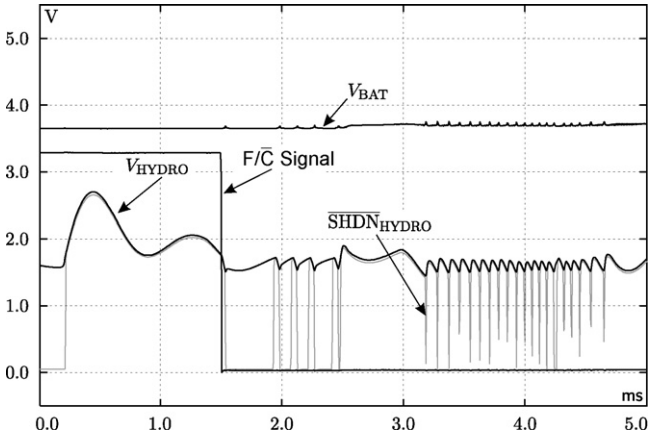

Fig. 13 – Hydrogenerator power conditioning waveforms when the charging process is started by the μ-controller, asserting the F/$\bar{C}$ signal low. After that, the power-conditioning subsystem keeps the hydrogenerator working at its MPP.

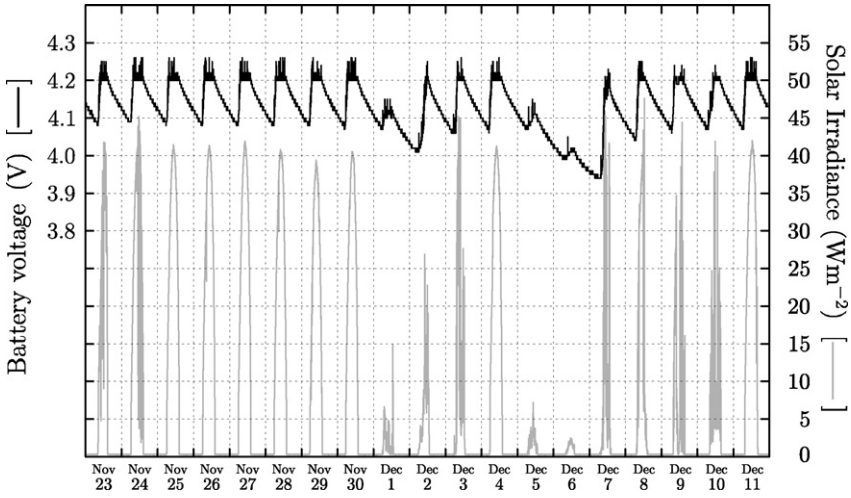

Fig. 14 – Behaviour of a 220 mAh battery in the MPWiNodeS WDAP during a winter 19-day evaluation period and using only the solar panel, transmitting data 60 s.

long battery lifetime, and, simultaneously, good harvesting efficiency.

3.2. *Data acquisition platform*

Targeted to PA applications, our WDAP comprises an analog interface based on a low-power analog-to-digital converter (AD7888BRZ from Analog Devices, USA), featuring eight analog inputs with 12-bit resolution (Fig. 7). External general-purpose sensors supply is accomplished by a separate DC–DC converter that is turned on only during the acquisition process.

Data from the power-conditioning subsystem, such as the signals from the energy harvesters and the battery voltage sample value, are handled in a different way. The pulses generated by each power conditioning block comparators' to control the corresponding boost converter are filtered before the analog-to-digital conversion takes place. This is done with an RC filter at the output of a low-power 4:1 multiplexer. The sampled battery voltage is taken by a separate analog channel, through a voltage divider enabled by an analog switch to save energy.

Table 2 – Sumarised results of MPWiNodeX, S and Z device evaluation

Partial result	Value
Hydrogenerator energy harvested	15 mAh (water flow = 0.5 $m^3\ s^{-1}$)
Wind generator energy (average 10 min)	32 mAh (averaged wind = 6.52 m/s)
Solar panel energy (worst case)	11 mAh (by integration)
Total energy harvested during evaluation	58 mAh
MPWiNodeX leakage current/efficiency	75 μA/83%
MPWiNodeS deep sleep/max current consumption[a]	110 μA/27 mA
MPWiNodeZ deep sleep	90 μA
MPWiNodeZ consumption 100%/10%/1% duty-cycle	39 mA/3.98 mA/0.469 mA
Sensors current consumption	1.2 mA

[a] All circuits ON:radio transmitting or receiving, sensors powered.

4. Experimental results

The energy harvesting methods were evaluated in two different devices (the -S and -Z variants, shown in Fig. 10). A MPWiNodeS device was installed outside our laboratory with the purpose of sending periodically solar irradiance, relative humidity, outside temperature and battery voltage data to a base station. This device is being used in a long-term evaluation of the proposed WDAP. Other similar device was used in the laboratory to an in-depth analysis of the power-conditioning subsystem waveforms. On the other hand, a MPWiNodeZ device was deployed in a vineyard as a ZigBee

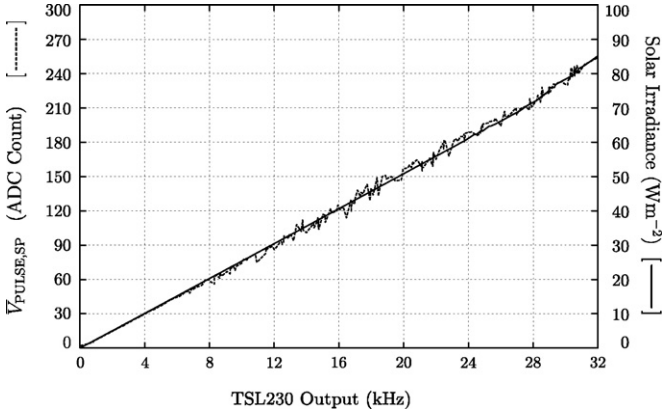

Fig. 15 – Solar irradiance sensor transfer function compared with the reference sensor (TSL230 from Texas Instruments, USA).

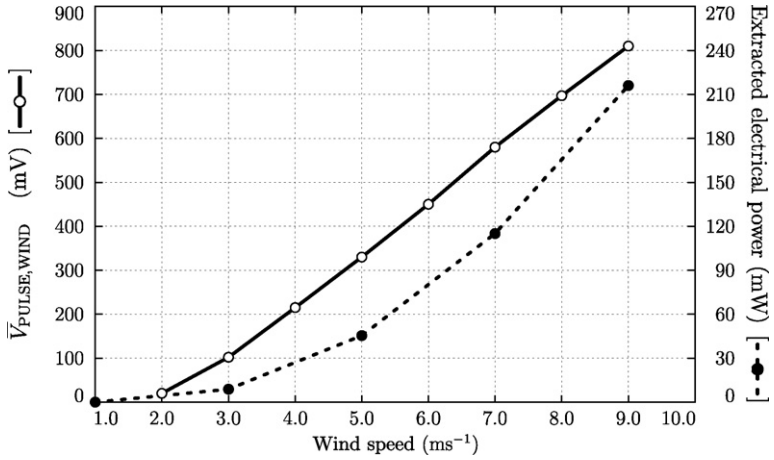

Fig. 16 – Wind speed sensor transfer function (solid line) and extracted electrical power (dashed line) obtained from the wind turbine evaluated in a wind tunnel.

network node to evaluate, in-field, the energy harvesters performance (Fig. 11).

The performance of the wind turbine was evaluated using a wind tunnel (4 m length, 0.4 m × 0.4 m cross-sectional area). Fig. 12 shows the relevant waveforms obtained with the correspondent power-conditioning block. The pulsed output was filtered to extract its DC value, yielding $\bar{V}_{PULSE,WIND}$. This evaluation was performed at various air speed values which has lead to the transfer function of Fig. 12. As can be seen, $\bar{V}_{PULSE,WIND}$ is proportional to wind speed, the linearised transfer function being approximately given by

$$\text{wind velocity} = \frac{1}{118.3}\,\bar{V}_{PULSE,WIND} + 2.15\,(\text{m/s}), \quad (4)$$

where $\bar{V}_{PULSE,WIND}$ is in mV. For speeds below approximately 2.1 m/s the voltage output from the turbine is not enough ($V_{WIND} < 2$ V) for turning on the boost converter, which indicates that this speed value is the minimum value that enables battery charging (as well as data from wind speed). As expected, the extracted electrical power (measured directly on the generator with a resistive load), follows a cubic-law, accordingly to (1).

Fig. 13 shows the behaviour of the hydrogenerator power-conditioning block. To illustrate the start charging procedure, the $F/\bar{C}$ signal is asserted low to select the charging mode. Until that, the hydrogenerator was operating without any electrical load. As can be seen, the battery starts charging and the power-conditioning block maintains the hydrogenerator working at its MPP (approximately at 1.5 V), by means of the $\overline{SHDN}_{HYDRO}$ signal.

For the field evaluation of the MPWiNodeS device, eight sensors were used for measuring air temperature (LM50B from National Semiconductor, USA), solar radiation (TSL230 and TSL251 from Texas Instruments, USA) and air relative humidity (HIH-3610 from Honeywell, USA) for creating a discharging profile and measure current consumption. In addition, data from solar radiation (obtained from the solar panel), wind speed (obtained from the wind turbine) and from battery were also transmitted to the base station for posterior analysis. The operation mode was deliberately set to be a relatively high duty-cycle, 10 s in a 60 s time-frame (16.7%). To get quicker results, a battery with a lower capacity (220 mAh) was used. The result of this evaluation period, regarding the battery behaviour, is shown in Fig. 14 where solar irradiance is also shown. The evaluation was performed over a period of variable weather (cloudy, foggy and bright, winter days). It can be seen that the battery stop charging control has keeping the battery voltage below 4.2 V, although it would be possible to go beyond that value.

The MPWiNodeZ device, as a ZigBee network router, was also evaluated. Table 2 summarises the obtained results. By gathering data from $\bar{V}_{PULSE,SP}$ and from the TSL230 solar radiation sensor, the transfer function illustrated in Fig. 15 was obtained.

5. Conclusions and final remarks

In principle, the energy required to permanently operate the wireless data acquisition nodes and routers in a large sensor network can be obtained by harvesting energy sources present in the environment. Our multi-powered platform was designed for applications in precision agriculture, and focuses on solar and kinetic energy sources (wind and water in pipes). The system that we built proves that the three harvesting methods suffice to supply a generic WDAP energy store. Even with low values of solar radiation, the combination of the three energy sources has supplied an energy of about 58 mAh, more than the 39 mAh required by network routers.

We have observed that the wind turbine is able to generate an important fraction of the harvested energy, in certain cases close to the needs of router nodes. Improving these generators may pay off in the future, particularly in applications where irrigation pipes are absent. At the opposite extreme one finds applications in greenhouses, hydroponic or aquaculture systems, in which case the wind is unlikely to play a major role but moving water in pipes is abundant, reversing the relative importance of wind turbines and hydro-generators.

Another novelty of our approach is the double functionality of the power management block, which in addition to its

usual role also doubles as a sensing device for the parameters that are usually monitored in agricultural environments. Our results and in particular Figs. 15 and 16 confirm that a coarse value of wind speed and solar irradiance can be measured by the corresponding energy harvester without the need for specific sensors. This is yet another advantage of the idea of harvesting from multiple energy sources: when the energy sources are related to parameters that the sensor network needs to measure, the amount of harvested energy may itself yield an estimate of the parameter, making conventional sensors unnecessary.

Several improvements to the basic ideas underlying this paper are possible, some of which are presently under study. The system could for example keep a record of each harvested energy source, and use it to predict its future availability. The use of Lithium batteries and ultracapacitors is also being evaluated as a way to slow down battery aging by absorbing the transient power and to minimise the issue described in Section 3.1.3.

Acknowledgements

The authors would like to thank Portugal Telecom Innovation (PT Inovação), which partially supported this work through the project "Wireless Farm". Electronic components samples for the developed prototypes were kindly supplied by Maxim Integrated Products, Inc., USA, Analog Devices, USA, and Coilcraft, USA (Inductors), which we gratefully acknowledge. We wish to thank Mr. António Domingos for helping us with wind speed data gathering.

REFERENCES

Betz, A., 1926. Wind-energie und ihre ausnutzung durch windmühlen. Bandenhoeck & Ruprect, Göttingen (Reprint 1994).

Cantatore, E., Ouwerkerk, M., 2006. Energy scavenging and power management in networks of autonomous microsensors. Microelectronics Journal 37, 1584–1590.

Chou, P.H., Park, C., 2005. Energy-efficient platform designs for real-world wireless sensing applications. In: ICCAD '05: Proceedings of the 2005 IEEE/ACM International conference on Computer-aided design, IEEE Computer Society, Washington, DC, USA, pp. 913–920.

Corke, P., Valencia, P., Sikka, P., Wark, T., Overs, L., 2007. Long-duration solar-powered wireless sensor networks. In: EmNets '07: Proceedings of the 4th Workshop on Embedded Networked Sensors, ACM, New York, NY, USA, pp. 33–37.

Dubois-Ferrière, H., Fabre, L., Meier, R., Metrailler, P., 2006. Tinynode: a comprehensive platform for wireless sensor network applications. In: IPSN '06: Proceedings of the Fifth International Conference on Information Processing in Sensor Networks, ACM, New York, NY, USA, pp. 358–365.

Fetcenko, M.A., Ovshinsky, S.R., Reichman, B., Young, K., Fierro, C., Koch, J., Zallen, A., Mays, W., Ouchi, T., 2007. Recent advances in NiMH battery technology. Journal of Power Sources 165, 544–551.

Hande, A., Polk, T., Walker, W., Bhatia, D., 2007. Indoor solar energy harvesting for sensor network router nodes. Microprocessors and Microsystems 31 (6), 420–432.

Hayashi, T., Li, Y., Hara, Y., 2005. Wind tunnel tests on a different phase three-stage Savonius rotor. JSME International Journal 48 (1), 9–16.

Jiang, X., Polastre, J., Culler, D., 2005. Perpetual environmentally powered sensor networks. In: IPSN '05: Proceedings of the 4th International Symposium on Information Processing in Sensor Networks. IEEE Press, Piscataway, NJ, USA, p. 65.

Mainwaring, A., Culler, D., Polastre, J., Szewczyk, R., Anderson, J., 2002. Wireless sensor networks for habitat monitoring. In: WSNA '02: Proceedings of the 1st ACM International Workshop on Wireless Sensor Networks and Applications, ACM, New York, NY, USA, pp. 88–97.

Maxim, 2000. Harnessing Solar Power with Smart Power-conversion Techniques. MAXIM Integrated Products, Inc., Application Note 364.

Morais, R., Fernandes, M.A., Matos, S.G., Serdio, C., Ferreira, P., Reis, M., 2008. A ZigBee multi-powered wireless acquisition device for remote sensing applications in precision viticulture. Computers and Electronics in Agriculture.

Moreenthaler, G.W., Khatib, N., Kim, B., 2003. Incorporating a constrained optimization algorithm into remote sensing/precision agriculture methodology. Acta Astronautica 53, 429–437.

Paradiso, J.A., Starner, T., 2005. Energy scavenging for mobile and wireless electronics. IEEE Pervasive Computing 4 (1), 18–27.

Park, C., Chou, P.H., 2006. Ambimax: Autonomous energy harvesting platform for multi-supply wireless sensor nodes. In: SECON '06: Proceedings of the 3rd Annual IEEE Communications Society on Sensor and Ad Hoc Communications and Networks, 1, pp. 168–177.

Priya, S., Chen, C., Fye, D., Zahnd, J., 2005. Piezoelectric windmill: A novel solution to remote sensing. Japanese Journal of Applied Physics 44 (3), 104–L107.

Rabaey, J.M., Ammer, M.J., da Silva, J.L., Patel, D., Roundy, S., 2000. Picoradio supports ad hoc ultra-low power wireless networking. Computer 33 (7), 42–48.

Raghunathan, V., Ganeriwal, S., Srivastana, M., 2006. Emerging techniques for long lived wireless sensor networks. IEEE Communications Magazine 44 (4), 108–114.

Raghunathan, V., Kansal, A., Hsu, J., Friedman, J., Srivastava, M., 2005. Design considerations for solar energy harvesting wireless embedded systems. In: IPSN'05: Proceedings of the 4th International Symposium on Information Processing in Sensor Networks. IEEE Press, Piscataway, NJ, USA, p. 64.

Roundy, S., Steingart, D., Frechette, L., Wright, P., Rabaey, J., 2004. Power sources for wireless sensor networks. Lecture Notes in Computer Science 2920, 1–17.

Shikha, Bhatti, T.S., Kothari, D.P., 2003. A new vertical axis wind rotor using convergent nozzles. Large Engineering Systems Conference on Power Engineering, 177–181.

Stafford, J.V., 2000. Implementing precision agriculture in the 21st century. Journal of Agricultural Engineering Research 76, 267–275.

Sweetser, D., Sweetser, V., Nemeth-Johannes, J., 7–9 February 2006. A Modular Approach to IEEE-1451.5 Wireless Sensor Development. In: SAS2006 – IEEE Sensors Applications Symposium, Houston, TX, USA, pp. 82–87.

Thomas, J.P., Qidwai, M.A., Kellogg, J.C., 2006. Energy scavenging for small-scale unmanned systems. Journal of Power Sources 159 (2), 1494–1509.

Wang, N., Zhang, N., Wang, M., 2006. Wireless sensors in agriculture and food industry—recent development and future perspective. Computers and Electronics in Agriculture 50, 1–14.

Wei, J., Zhang, N., Wang, N., Lenhert, D., Neilsen, M., Mizuno, M., 2005. Use of the "smart transducer" concept and IEEE 1451 standards in system integration for precision agriculture. Computers and Electronics in Agriculture 48, 245–255.

Ying, T.K., Gao, X.P., Hu, W.K., Wu, F., Noréus, D., 2006. Studies on rechargeable NiMH batteries. International Journal of Hydrogen Energy 31, 525–530.

Zhang, J., Yu, J., Cha, C., Yand, H., 2004. The effects of pulse charging on inner pressure and cycling characteristics of sealed Ni/MH batteries. Journal of Power Sources 136, 180–185.

Raul Morais dos Santos graduated in Electrical Engineering from the University of Trs-os-Montes and Alto Douro (UTAD), Portugal in 1993. He obtained the M.Sc. degree in Industrial Electronics in 1998 from the University of Minho, Portugal and the Ph.D. degree in Microelectronics in 2004 from the UTAD. Presently, he is an Assistant Professor in the Department of Electrical Engineering, UTAD. He is also a researcher in the Signal Processing and Biotelemetry group at the Center for the Research and Technology of Agro-Environment and Biological Sciences of UTAD (CITAB/UTAD), and he is involved in the development of instrumentation solutions and mixed-signal sensing interfaces for agricultural applications. He is also leading the CITAB effort of implementing an agricultural remote sensing network in the Demarcated Region of Douro, a UNESCO Heritage Site.

Samuel Ricardo G. Matos graduated in Electrical Engineering from the University of Trás-os-Montes e Alto Douro (UTAD), Portugal in 2005. He is pursuing its Ph.D. degree in Electrical Engineering developing the concept of highly flexible smart acquisition devices.

Miguel Alves Fernandes graduated in Electrical Engineering from the University of Trs-os-Montes e Alto Douro (UTAD), Portugal in 2005. He is pursuing its Ph.D. degree in Electrical Engineering exploring and characterising the concept of the wireless farm.

António Luis G. Valente graduated in Electrical Engineering from the University of Trs-os-Montes and Alto Douro (UTAD), Portugal in 1994. He obtained the M.Sc. degree in Industrial Electronics in 1999 from the University of Minho, Portugal and the Ph.D. degree in Microelectronics in 2004 from the UTAD. Presently, he is an Assistant Professor in the Department of Electrical Engineering, UTAD. He is also a researcher at the CITAB/UTAD and he is involved in the research of silicon microsensors for agriculture.

Salviano F.S.P. Soares graduated in Electrical Engineering from the University of Trás-os-Montes e Alto Douro (UTAD), Portugal in 1991. He obtained the M.Sc. degree in Electronics and Telecommunications in 1995 from University of Aveiro (UA), Portugal, and the Ph.D. degree in Electrical Engineering in 2003 from UA. Presently, he is an Assistant Professor an Department of Electrical Engineering, UTAD, and also a researcher at the CITAB/UTAD. His main interest area is digital signal processing.

Paulo J.S.G. Ferreira is a full professor at the Departamento de Electrónica, Telecomunicações e Informtica/IEETA, University of Aveiro, Portugal. He was an associate editor of the *IEEE Transactions on Signal Processing*, and is currently a member of the editorial board of the *Journal of Applied Functional Analysis* and an Editor-in-Chief of *Sampling Theory in Signal and Image Processing*. He co-edited with John J. Benedetto the book *Modern Sampling Theory: Mathematics and Applications*. His current research interests include sensors and coding, as well as sampling and signal reconstruction.

Manuel J. Cabral S. Reis received the Ph.D. degree in Electrical Engineering and the M.Sc. degree in Electronics and Telecommunications from the University of Aveiro, Portugal. Currently he is Assistant Professor in the Department of Engineering of University of Trs-os-Montes e Alto Douro (UTAD), Portugal. He is also a researcher at the CITAB/UTAD, where he is the director of Signal Processing and Biotelemetry group. His research interests are in the area of signal processing, and include modelling and approximation, and problems such as sampling, interpolation, and signal reconstruction.